JOURNAL OF MATERIALS SCIENCE 26 (1991) 749–755

Corrosion and wetting behaviour of metals and steels with molten alkali carbonates

J. M. FISHER, P. S. BENNETT
Johnson Matthey Technology Centre, Blount's Court, Sonning Common, Reading RG4 9NH, UK

The corrosion and wetting behaviour of metals and steels with molten alkali carbonates is of particular interest for the design of molten carbonate fuel cells. Such cells, operating at 650 °C with a lithium and potassium carbonate electrolyte, offer a very corrosive medium for fuel cell components.

Static corrosion tests under simulated anode conditions have shown that rhodium, ruthenium, platinum, palladium, silver, gold, Nickel 200 and Monel 400 exhibit no measurable corrosion over a 100 h period. Copper, Kanthal and Fecralloy exhibit good resistance with thin protective oxide layers. Stainless steels show less resistance to attack with thicker more permeable oxide coatings being formed.

In addition, contact angle measurements indicate that copper, gold, silver and ruthenium demonstrate appreciable non-wetting under a H_2–CO_2 atmosphere. Steels are substantially wetted.

1. Introduction

The molten carbonate fuel cell offers an attractive means of converting the chemical energy of a fuel and an oxidant to electrical energy [1]. In common with all fuel cells, the conversion efficiency is not subject to the limitations of the Carnot heat cycle. The operating temperature of molten carbonate fuel cells is generally 650 °C and the reaction kinetics are significantly faster than in lower temperature cells. In addition, the ohmic resistance of the usual 62:38 mol % lithium carbonate: potassium carbonate electrolyte is relatively low and efficiencies in the order of 50–55% have been reported [2].

A schematic diagram of a molten carbonate fuel cell is shown in Fig. 1. Typically both the anode and cathode are made from nickel, although alternative materials are undergoing trial [3, 4]. During operation, the oxidizing atmosphere at the cathode rapidly converts the nickel cathode to nickel oxide. The carbonate electrolyte is supported in a matrix of lithium aluminate and this is known as the "electrolyte tile". The separator plate and current collector are generally made from stainless steel. The fuel cell stack consists of repeating layers of "electrolyte tile", cathode, current collector, separator plate and anode (Fig. 2).

The carbonate ion itself takes part in the electrode reactions, and the melt remains constant in composition by a continuous transfer of carbonate ion from cathode to anode.

Anode: $H_2 + CO_3^{2-} \rightarrow H_2O + CO_2 + 2e^-$

$CO + CO_3^{2-} \rightarrow 2CO_2 + 2e^-$

Cathode: $CO_2 + \frac{1}{2}O_2 + 2e^- \rightarrow CO_3^{2-}$

Overall cell reaction: $H_2 + \frac{1}{2}O_2 \rightarrow H_2O$

The corrosion behaviour of metals and steels with molten alkali carbonate is of particular interest for the design and construction of such fuel cells. The high operating temperature and the alkali carbonate electrolyte provide a very aggressive medium for components such as electrodes, separator plates, direct internal reforming catalysts, etc. If molten carbonate fuel cells are to succeed commercially, the problems of component corrosion will have to be overcome.

In addition, limited information is available in the literature concerning materials wettability. This would be useful for the design of, e.g. electrodes or non-wetted direct internal reforming catalysts.

Parameters such as the purity of the carbonate, the gas atmosphere and the temperature are of importance in determining corrosion and wetting behaviour, and the literature in this area is often confusing because of differing experimental conditions. The present study describes a wide survey of the corrosion and wetting behaviour of metals and steels with molten carbonate under anode conditions.

2. Experimental details

Static corrosion tests were carried out in the apparatus illustrated in Fig. 3. The 62 mol % Li_2CO_3 and 38 mol % K_2CO_3 eutectic was used throughout and the tests were conducted at 650 °C with an inlet gas stream of 68% H_2, 17% CO_2 and 15% H_2O.

Lithium carbonate and potassium carbonate (BDH AnalaR grade) were purified prior to use (to remove traces of oxide and hydroxide) by passing O_2-free CO_2 through the molten mixture for 24 h. Preliminary experiments indicated gold to be extremely corrosion

0022–2461/91 $03.00 + .12

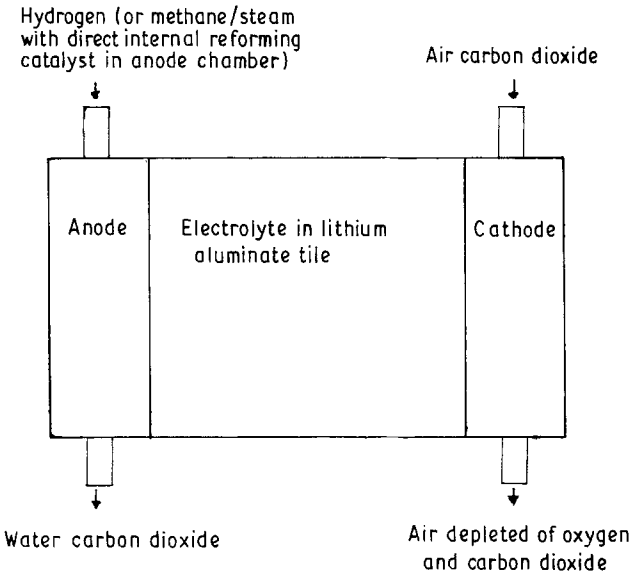

Figure 1 Schematic diagram of a single molten carbonate fuel cell.

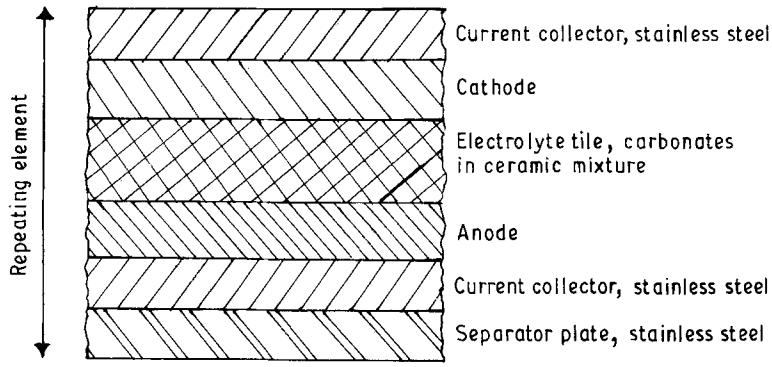

Figure 2 Repeating element of components necessary for a fuel cell stack.

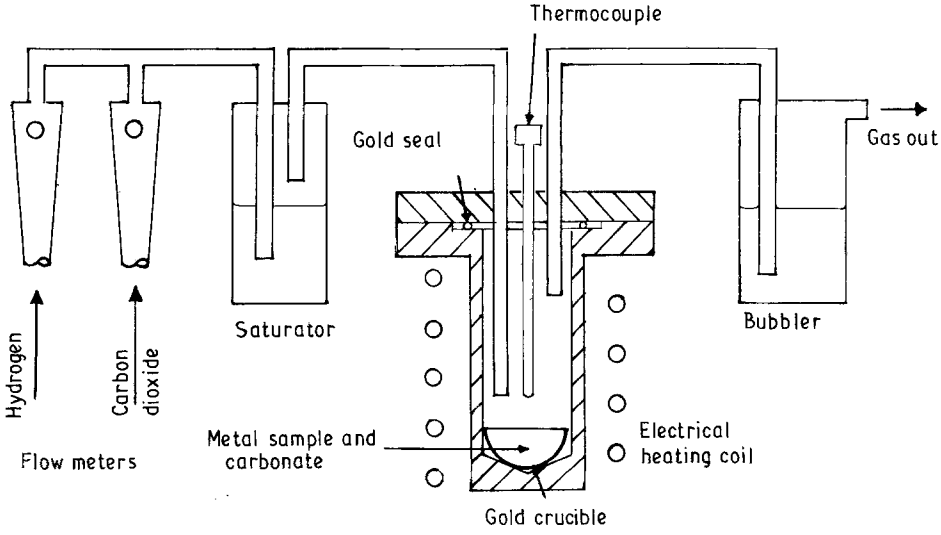

Figure 3 Corrosion test apparatus.

resistant under test conditions, so the samples and the carbonate were contained in small gold crucibles.

Samples were tested, where possible, as foil coupons ($1 \times 2\ cm^2$) and the compositions of some of the more unusual materials are given in Table I. After degreasing in acetone and weighing, the coupons were inclined across the crucible with one end of the coupon touching the bottom of the crucible and the other end the top of the crucible. Carbonate (0.5 to 0.6 g) was added which, when molten, was sufficient to submerge the coupon by one-third to one-half. The crucible and contents were heated under CO_2 to melt the carbonate and anchor the sample, and after cooling the crucible was placed inside the flanged stainless steel test chamber.

After testing, the coupons were washed to remove the carbonate and reweighed. The steels and some of the metals were studied by scanning electron microscopy (SEM). Pieces of the corroded and uncorroded samples were mounted on small aluminium stubs with

TABLE I Alloy-metal compositions

Material	Elemental composition (%)													
	C	Cu	Pb	Zn	Fe	Mn	Cr	Al	Sn	V	W	Mg	P	Si
Brass		60.0	1.5	38.5										
Silver steel	1.2				98.0	0.4	0.4							
Lead-free brass		70.0		29.0					1.0					
Arne tool-steel	0.9				96.8	1.2	0.5			0.1	0.5			
Dural		4.5			0.6	0.4		93.6				0.4		0.5
Phosphor-bronze		79.5	9.6						10.2				0.7	

carbon conductive cement and were then coated with carbon (40 nm). Large area analysis using energy-dispersive X-ray analysis was carried out on the standards and in triplicate on the corroded samples. The corroded samples were also mounted on Araldite and polished to show the cross-section.

Contact angles were measured using a standard hot stage microscope with vacuum chamber, workstage, microscope and vacuum pumping equipment. Metal coupons (approximately $2 \times 1\ cm^2$) were abrased with emery paper and then polished using diamond paste to 1 μm. The samples were degreased in acetone and loaded onto the microscope workstage. A piece of purified carbonate (~ 0.002 g) was placed on top of the sample. The chamber was evacuated to 4×10^{-2} mbar and then back-filled with H_2:CO_2 80:20. This gas mixture was purged through the system throughout the test ($50\ cm^3\ min^{-1}$). After at least ten minutes stabilization, the sample was heated and the contact angle was measured on both sides of the carbonate drop. The tests were duplicated.

TABLE II Weight changes after corrosion with carbonate Li_2CO_3:K_2CO_3 62:38 mol %, 650 °C, inlet gas: 68% H_2, 17% CO_2 and 15% H_2O.

Material	Test Duration (h)	Weight change (g)	Weight change ($g\ cm^{-2}$)
347 Stainless Steel	90.0	+ 0.022	0.003
Incoloy 825	92.5	− 0.020	− 0.003
310 Stainless Steel	92.1	+ 0.023	0.005
316 Stainless Steel	90.0	+ 0.007	0.002
321 Stainless Steel	90.1	+ 0.009	0.002
304 Stainless Steel	90.1	+ 0.017	0.002
Silver Steel	92.6	+ 0.003	0.077
Arne tool steel	93.2	+ 0.021	0.057
Brass	92.6	− 0.023	0.725
Lead-free brass	93.2	− 0.095	0.577
Phosphor-bronze	97.0	+ 0.020	0.202
Dural®	97.0	Material totally destroyed	
Fecralloy®	92.5	+ 0.013	0.004
Kanthal	92.5	+ 0.004	0.001
Monel 400	90.0	+ 0.014	0.002
Nickel 200	90.1	+ 0.002	0.001
Aluminium	93.2	Material totally destroyed	
Copper	92.4	+ 0.001	0.001
Rhodium	93.6	− 0.002	− 0.001
Ruthenium	93.6	+ 0.002	0.001
Platinum	93.1	+ 0.002	0.001
Palladium	93.1	+ 0.004	0.001
Silver	93.6	+ 0.001	0.000
Gold	90.2	0.000	0.000

3. Results and discussion

The weight changes after 100 h corrosion testing are given in Table II. Not surprisingly, the aluminium and Dural® samples were completely destroyed during the test. The samples of brass, lead-free brass and phosphor-bronze suffered substantial visible damage and significant weight change. These materials were not studied further. The steel samples, the copper, Fecralloy and Kanthal showed less visible damage and were all examined by SEM.

Two general points were noteworthy. Firstly, the corrosion was asymmetric. The depth of the corrosion layer on each side of the foil or sheet varied. The maximum corrosion depth is reported in Table III. Secondly, in many cases, the corrosion layer itself was not homogeneous.

All of the steels appear to have been corroded in a similar way. The surface analysis figures (Table III) show an increase in iron and a decrease in nickel and chromium as compared to the uncorroded "standard" samples. The corrosion layer was not homogeneous: the surface was iron rich with a thin layer beneath consisting entirely of chromium. This suggests an iron-oxide rich outer layer and an inner chromium oxide layer. SEM micrographs are shown in Figs 4 to 12. The 310 stainless steel (Fig. 4) has a more compact corrosion layer, whilst the 347 and 304 steels (Figs 5 and 6) have a voluminous and possibly more permeable oxide layer. The 316, 321 and 310 stainless steels appear to have the best resistance to corrosion.

The silver steel has a reasonably compact corrosion layer, whilst that on the tool steel is much wider (Figs 9 and 7). Incoloy 825 was attacked in a manner not dissimilar to the steels with a decrease in the surface concentration of nickel.

The micrographs of Fecralloy® and Kanthal are shown in Figs 11 and 12. These materials appear to be much more resistant to attack than the steels, although the corrosion is quite uneven in places. The surface analyses show a large increase in aluminium. Presumably a protective alumina or lithium aluminate layer has been formed. Copper has only a thin corrosion layer, probably an oxide coating.

Samples of Nickel 200, Monel 400, rhodium, ruthenium, platinum, palladium, silver and gold were visibly untouched after 100 h corrosion testing. The weight changes observed for these materials were

TABLE III 24 h and 100 h "Wet" corrosion test results for steels
(Li_2CO_3:K_2CO_3 62:38 mol %, 650 °C, inlet gas: 68% H_2, 17% CO_2, 15% H_2O)

	Surface Analyses (wt %)																			Maximum depth of corrosion layer, (μm)	
	Uncorroded						24 h corrosion						100 h corrosion								
Material	Al	Cu	Cr	Mn	Fe	Ni	Al	K	Cr	Mn	Fe	Ni	Al	Cu	K	Cr	Mn	Fe	Ni	24 h	100 h
Fecralloy®	8.3		16.0		76.0	0.3	13.3	3.2	20.0		63.2	0.3	12.0		1.3	14.0	0.2	71.1	1.4	6.5	11.8
Kanthal	9.5		20.0	0.4	69.0	0.5	26.0		18.0	0.7	54.6	0.4	38.0		0.2	16.0	0.6	44.7	0.5	2.3	6.2
Incoloy 825			22.0	0.4	30.0	48.0		3.3	55.0	0	26.0	16.0			0.4	36.0	0.8	55.0	7.8	5.6	22.0
304 SS			19.0	1.2	70.0	9.4			2.4	2.6	95.0	0.4			0.2	1.4	1.5	97.0	0.4	19.5	19.5
316 SS			18.0	1.7	67.9	13.0			2.4	1.7	95.0	1.0			1.1	4.3	1.7	92.0	1.4	8.5	12.0
321 SS			18.0	1.3	71.0	9.3			4.4	4.2	87.1	4.2				1.1	3.0	96.0	0.2	8.5	12.0
347 SS			18.0	1.6	71.0	9.5		1.9	11.6	0.2	76.2	9.6			1.5	2.3	2.8	93.0	0.4	7.9	15.8
310 SS			25.0	1.8	53.0	20.0		18.0	43.0	7.1	31.0	0.2			4.9	24.0	2.7	66.5	1.8	14.3	19.0
Tool steel			0.7	1.5	97.4	0.3										0.6		96.5	2.5		27.5
Silver steel			0.6	0.5	98.4	0.5									0.5	0.5		98.5	0.5		15.0
Copper		99.9												98.5							3.0

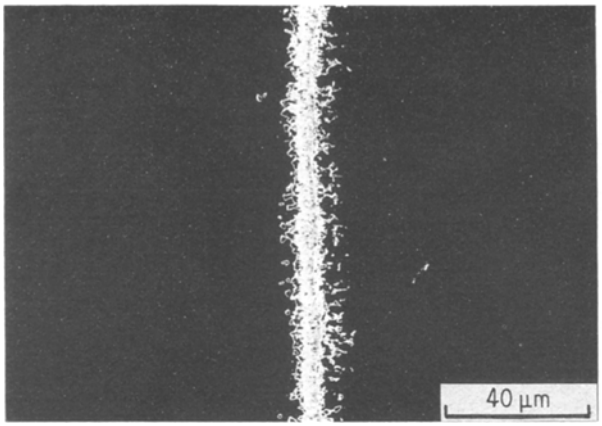

Figure 4 Edge view of "corroded" 310 stainless steel.

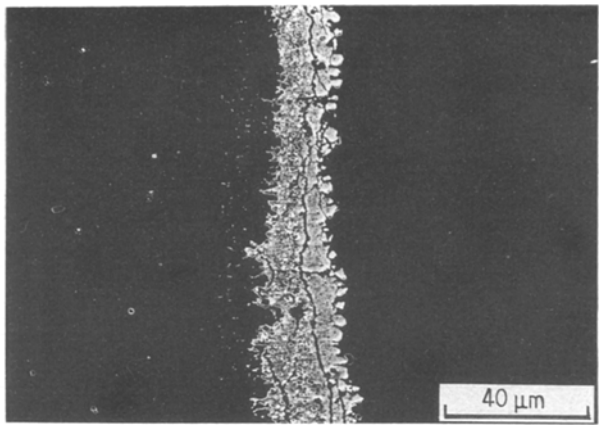

Figure 7 Edge view of "corroded" tool steel.

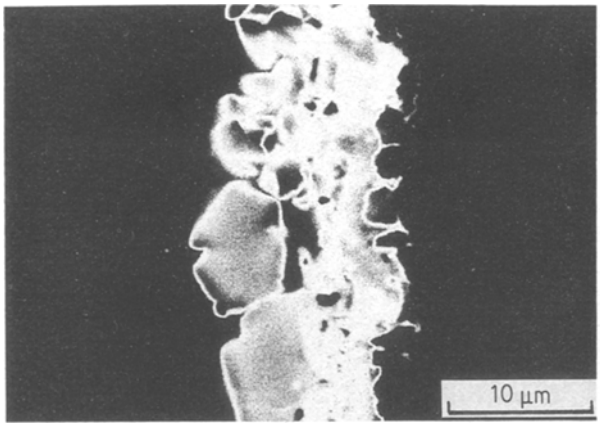

Figure 5 Edge view of "corroded" 347 stainless steel.

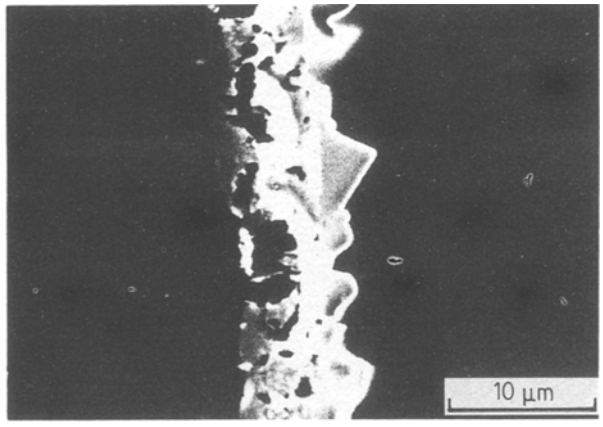

Figure 8 Edge view of "corroded" 321 stainless steel.

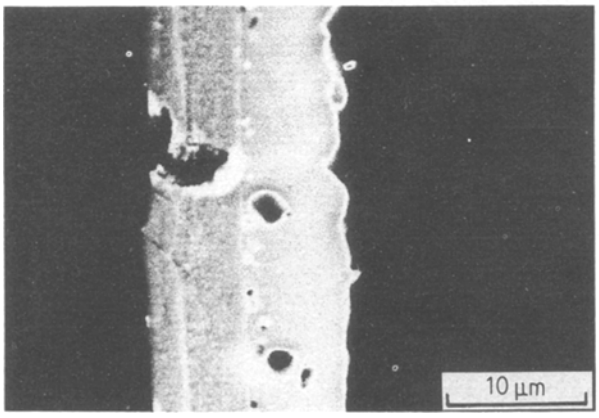

Figure 6 Edge view of "corroded" 304 stainless steel.

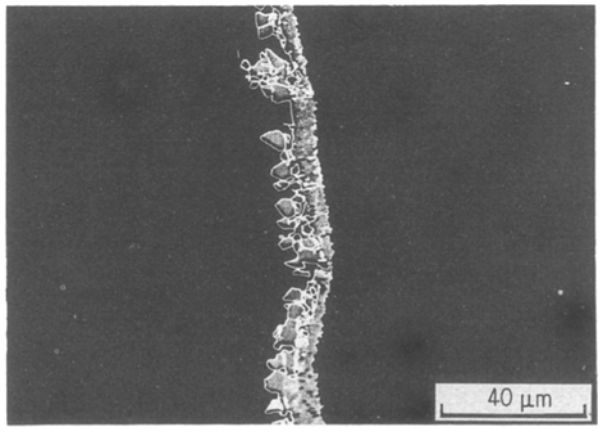

Figure 9 Edge view of "corroded" silver steel.

almost negligible (Table II). They were therefore not studied by SEM.

The results for platinum and silver appeared surprising in view of the fact that corrosion under carbon dioxide had previously been reported [5]. In the current work, however, hydrogen was also included in the gas atmosphere, and no trace of the previously reported lithium platinate was found by X-ray photoelectron spectroscopy (XPS).

The 100 h corrosion test was repeated for platinum and silver in an oxidizing atmosphere of 50% carbon dioxide, 50% air. Under these conditions silver had visibly dissolved in the carbonate and some had plated out on to the bottom of the crucible. The corrosion of silver under oxidizing conditions is consistent with data in the literature [6]. The platinum sample had changed colour, and when studied by XPS the surface layer was found to be Li_2PtO_3. Platinum is reported in the literature [7] to form Li_2PtO_3 when heated with Li_2CO_3 to 650 to 1000 °C under oxygen. Silver and platinum are therefore considered to be unsuitable for use at the cathode side of the fuel cell.

Contact angle measurements under H_2:CO_2 are given in Table IV. Preliminary experiments under hydrogen (not reported) suggested that the steels substantially wetted, and these materials were not tested

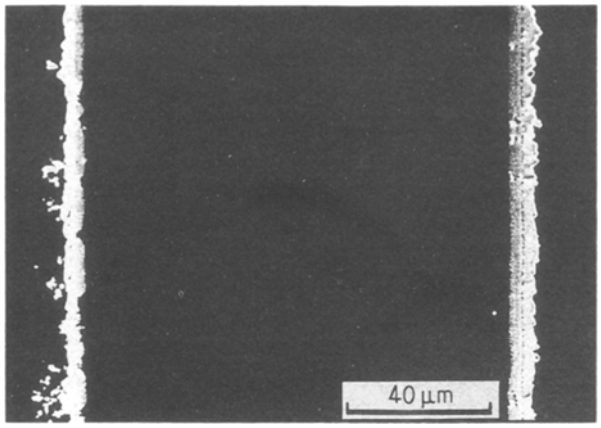

Figure 10 Cross-sectional view of "corroded" 316 stainless steel.

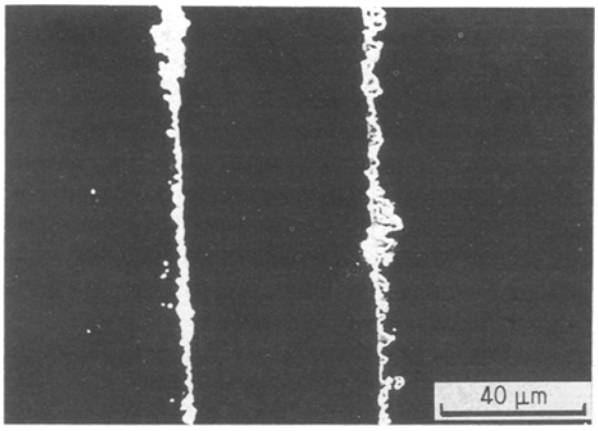

Figure 11 Cross-sectional view of "corroded" Fecralloy®.

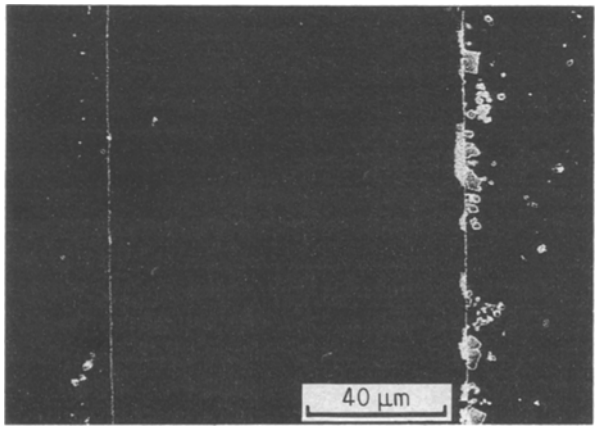

Figure 12 Cross-sectional view of "corroded" Kanthal®

under H_2:CO_2. The wetting of the steels is presumably due to oxide layers [8]. When a series of metal oxides were tested (as pressed sintered discs) complete wetting was observed almost immediately the carbonate melted. The presence of CO_2 in the gas stream prevents possible breakdown of the carbonate ($CO_3^{2-} \rightarrow CO_2 + \frac{1}{2}O_2^{2-}$) and simulates more closely the anode gas stream. It can be seen from Table IV that gold, silver, ruthenium and copper have contact angles of greater than 60°, significantly non-wetting. These materials also showed good resistance to corrosion. Materials which are non-wetting may be useful to prevent electrolyte loss by "wicking" and also to modify the wetting behaviour of electrodes. The surface finish of the samples tested for wetting behaviour was found to be of importance. For example when the surface of a non-wetting sample was roughened (e.g. by grit blasting) the contact angle was found to increase dramatically. This phenomenon has been reported previously with other systems [9, 10].

TABLE IV Contact angles measured at 650 °C with inlet gas H_2:CO_2 80:20

(Li_2CO_3:K_2CO_3 62:38 mol %, measurements reproducible to within ± 2° unless otherwise noted)

Material	Contact angle
Rhodium	43[a]
Ruthenium	92
Gold	63
Silver	63
Monel 400	43
Nickel 200	50[b]
Palladium	41
Copper	88
Platinum	49

[a] reproducibility ± 4°.
[b] carbonate migration across metal surface.

4. Conclusions

During early work on molten carbonate fuel cells, platinum, palladium and palladium–silver alloys were used as anode materials [11–13] but they were rejected on the grounds of cost, however, the platinum group metals do offer excellent corrosion resistance to molten carbonate. In addition, gold, silver and ruthenium are not wetted by the carbonate. They could possibly be used as electrolyte barriers.

Nickel 200, Kanthal and Fecralloy have shown good resistance under anode conditions. This is in accord with recently published Japanese work [14] where aluminized steels and nickel were found to be corrosion resistant under fuel gas.

The oxide coating on the Kanthal and Fecralloy is more compact and thinner than the oxide coating on the stainless steel. If Kanthal and Fecralloy show good resistance under cathode conditions, they may find uses as materials for separator plates.

References

1. J. R. SELMAN and L. G. MARIANOWSKI, in "Molten Salt Technology" (Plenum Press, New York, 1982) p. 323.
2. L. PAETSCH, P. S. PATEL, H. C. MARU and B. S. BAKER, Program and Abstracts Fuel Cell Seminar, Tucson, Arizona 1986, p. 143.
3. R. D. PIERCE, J. L. SMITH and G. H. KUCERA, *Prog. Batteries Solar Cells* **6** (1987) 159.
4. S. E. WEBER, P. PETTY and A. C. KHANDKAR, presented at 15th Workshop on MCFC Technology.
5. G. J. JANZ, A. CONTE and E. NEUENSCHWANDER, *Corrosion* **19** (1963) 292.
6. I. TRACHTENBERG and D. F. COLE, in "Fuel Cell Systems 2", edited by B. S. Baker (*Advances in Chemistry* **90**) (American Chemical Society, New York, 1969).

7. J. J. SCHEER, A. E. VAN ARKEL and R. D. HEYDING, *Can. J. Chem.* **33** (1961) 683.
8. G. K. MOISEEV and G. K. STEPANOV, *Electrochem. Molten Solid Electrolytes* **5** (1967) 101.
9. R. N. WENZEL, *Ind. Eng. Chem.* **28** (1936) 988.
10. M. G. NICHOLAS, R. M. CRISPIN and D. A. FORD, in "Ceramic Surfaces and Surface Treatments", edited by R. Morrell and M. G. Nicholas (British Ceramic Society Proceedings, British Ceramic Research Association **34**) 1984.
11. G. H. J. BROERS and J. A. A. KETELAAR, *Ind. Eng. Chem.* **52** (1960) 303.
12. L. G. MARIANOWSKI, J. MEEK, E. B. SCHULTZ and B. S. BAKER, in Proceedings of the 17th Annual Power Sources Conference, Red Bank, New Jersey 1969 (PSC Publications Committee, Red Bank, Jersey) p. 72.
13. J. T. COB and L. F. ALBRIGHT, *J. Electrochem. Soc.* **115** (1968) 2.
14. K. NAKAGAWA, T. ISOZAKIK and S. KIHARA, *Bostoku Gijutsu* **36** (1987) 438.

Received 11 August 1989
and accepted 19 February 1990